Observation of a Kink Soliton on the Surface of a Liquid

Bruce Denardo,[a] William Wright, and Seth Putterman
Department of Physics, University of California, Los Angeles, California 90024-1547

Andrés Larraza
Department of Physics, Naval Postgraduate School, Monterey, California 93943
(Received 16 November 1989)

When a long channel of shallow liquid is driven parametrically, there can occur a 180° kink in the phase of the fundamental cross mode of the surface. The kink is stable and localized, and is nonpropagating in the limit where the system is uniform. The weakly nonlinear theoretical description is a damped driven nonlinear Schrödinger equation supplemented with second harmonics. The kink is a robust state even at amplitudes where the perturbation expansion leading to this equation is unjustified.

PACS numbers: 43.25.+y, 47.35.+i

We have observed a kink in the phase of surface wave oscillations on a shallow liquid in a parametrically driven rectangular channel.[1] The stability of this state suggests that it is a physical realization of a soliton. Figure 1 shows a perspective view of a mathematical idealization of the kink, which is a localized transition between two uniform domains that are 180° out of phase. A breather soliton has been observed in a similar system with deep liquid.[2] The experiments reported here were motivated by our observation of a kink in a parametrically driven pendulum lattice.[3]

The best experimental evidence for the solitary nature of the kink is its slow but reproducible drift motion in a channel that is slightly tilted. Figure 2(a) shows the profile (maximum and minimum vertical surface displacement) as the kink drifted by a fixed probe, which was located at the longitudinal midpoint and near one wall of the channel. The kink moves to shallower regions until it stops in the vicinity of the end wall. The minimum peak-to-peak amplitude is not strictly a node as in Fig. 1 at $x=0$, but for convenience we will refer to it as such. Figure 2(c) is a graph of the drift velocity as a function of the angle of inclination of the channel. The drift velocity was measured by timing the transit of the cusp (Fig. 2) as it moved between two probes located

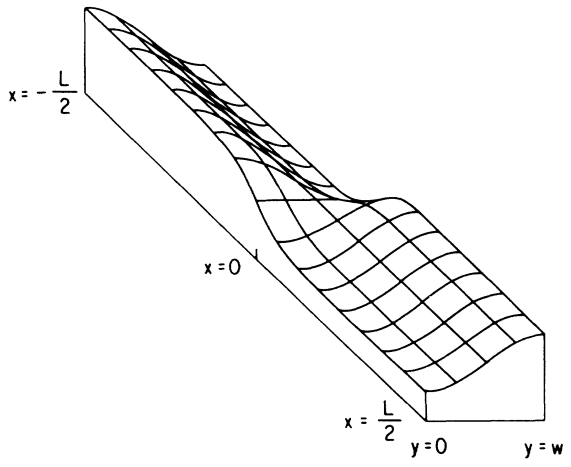

FIG. 1. Perspective view of a mathematical approximation of the observed kink. The vertical surface displacement is proportional to $\tanh(\alpha x)\cos(\pi y/w)$.

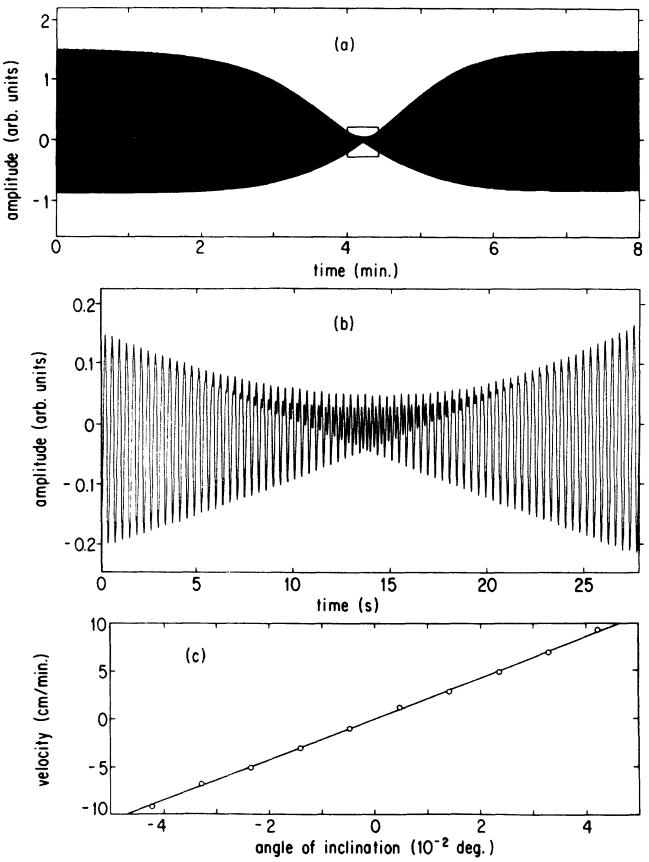

FIG. 2. Drift motion of a kink: (a) profile at a fixed probe, (b) enlargement of the vertical surface displacement in the nodal region, and (c) drift velocity as a function of the angle of inclination of the channel. The drive parameters are 5.37 Hz and 0.54 mm.

symmetrically about the longitudinal midpoint of the channel. The slope of the best-fit line is 3.5 cm/sdeg. For a magnitude of the tilt angle greater than 0.045°, and "antikink" (180° out of phase relative to the original kink) emerges from the shallower end, and eventually inhibits the drift motion of the kink.

For surface waves of small amplitude the channel is a resonator characterized by the number of displacement nodes (n_x,n_y) perpendicular to the longitudinal and transverse directions, respectively. The even spacing between nodes is determined by the global geometry, viz., the walls. The kink, however, can occur at any location. It can be viewed as a large-amplitude (1,1) mode in which the transverse nodal line has become decoupled from the end walls of the channel as a result of the flattening of the profile. Similarly, a kink-antikink pair can be viewed as a large-amplitude (2,1) mode.

The channel is made of acrylic, and has inner width $w=5.71$ cm and inner length $L=76.2$ cm. The data reported here are for ethyl alcohol with a depth of $h=1.00$ cm in a covered channel. We have also observed kinks in either glass or acrylic channels of half the width and length with either alcohol or water, although a wetting agent must be added to water. To overcome dissipation and achieve a steady state, as well as to specify the frequency of response, we oscillate the channel vertically with a shake table. This was made by attaching an aluminum plate to the cone of an 18-in. loudspeaker, and using springs to offset the weight of the table and channel. The loudspeaker rests on a tripod which permits careful adjusting of the angle of inclination of the channel. The angular position of a wrench attached to one of the leveling bolts was calibrated to yield this angle. Because precise frequency control is required, a synthesizer is used to drive the shake table. Each probe is a pair of vertical wires separated by 4 mm, and connected to a high-frequency (2 kHz) voltage source. The resistance (10 MΩ) across the probe decreases as the level of liquid rises. Hence, the voltage across a small series resistor (40 kΩ) varies linearly with the surface height. The high frequency is removed from this signal by a lock-in amplifier.

We create a kink by imparting to the channel an angular impulse about any vertical axis through the channel, as long as the axis is not near the end walls. The node of the kink forms at the axis, and then gradually drifts due to nonuniformities. A kink can be moved by "dragging" the node with a narrow spatula that is inserted parallel to the channel. Using spatulas to bring a kink and antikink near each other, we have observed a repulsive interaction, which is so strong that the annihilation of a pair has never occurred without complete destruction of the cross mode. A repulsive force also exists between a breather and antibreather. These forces are in qualitative accord with Bernoulli's law.[2]

Profiles of large- and small-amplitude kinks are shown in Fig. 3. The data were taken with a probe parallel to and one meniscus length (2 mm) from a wall. To obtain the data, we constructed the cover of the channel to be similar to a slide rule, with the probe attached to the slide. Because the kink is sensitive to nonuniformities of the channel, a thin isosceles-triangular block is used to immobilize the kink for the purpose of taking the measurements in Fig. 3. The block is made of acrylic, and has height 1 mm, length 10 cm, and width equal to that of the channel. The probe was statically calibrated at the beginning and end of each data-gathering session. The slope of the calibration graph was stable to ±2% for sessions of typically 5 h.

Figure 4 is a graph of the drive-plane region in which the kink and (1,1) mode exist. The response frequency is

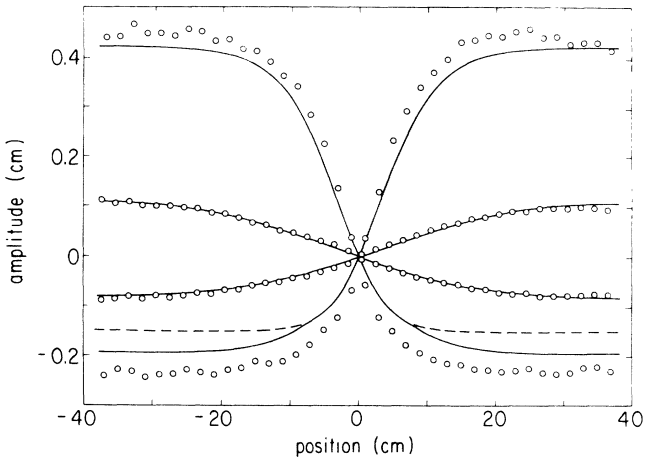

FIG. 3. Profiles of large- and small-amplitude kinks. The points are experimental and the curves are theoretical. The drive parameters are 5.37 Hz and 0.52 mm for the large-amplitude case, and 5.23 Hz and 0.46 mm for the small-amplitude case.

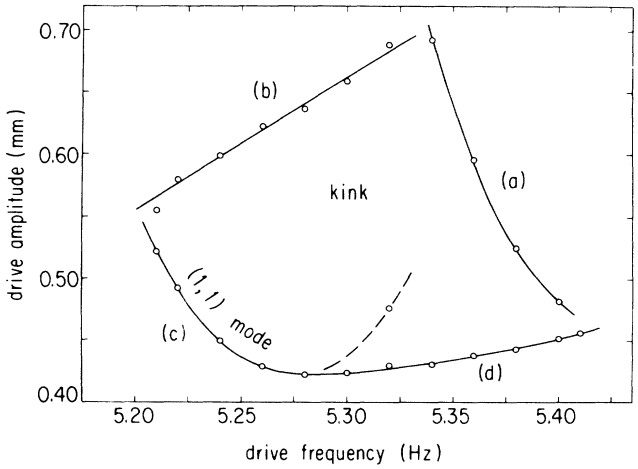

FIG. 4. Drive-plane portrait. The kink and (1,1) mode exist in the regions shown.

precisely half the drive frequency. The drive amplitude was measured with an accelerometer (Brüel and Kjaer 4332). Above boundary a, there appear modulations whose wavelength roughly equals the width of the channel. Above boundary b, the node is repelled from, rather than attracted to, the apex of the triangle. The node drifts to a position near one end of the channel and eventually disappears in the end. Below boundary c the kink decays to the rest state from a small amplitude ($\lesssim 0.5$ mm). This boundary is the well-known threshold for parametric excitation, which is theoretically a hyperbola in the drive plane.[4] The minimum in boundary c occurs at twice the linear frequency of the (1,1) mode. We have roughly extended the curve (dashed line) to frequencies greater than this value. The datum here was obtained by starting with the liquid at rest, imparting a small angular impulse to the channel, and determining the minimum drive amplitude for which the amplitude of the wave grew. Each point of boundary d corresponds to the common point of the stable and unstable branches of a parametric steady-state response curve,[4] where the amplitude jumps from a finite value to zero.

To theoretically describe the kink, we consider a modulation of the fundamental cross mode of a channel of liquid with the dimensions and coordinates as shown in Fig. 1, where $L \gg w$. The modulation is assumed to be slowly varying in space and time. On the weakly nonlinear level, the surface height is[5]

$$\zeta(x,y,t) = [\zeta_1(x,t)e^{i\omega t} + \text{c.c.}]\cos(ky) + [\zeta_2(x,t)e^{2i\omega t} + \text{c.c.} + \zeta_2^{(0)}(x,t)]\cos(2ky)\,, \tag{1}$$

where ω is the angular frequency of the wave, and $k = \pi/w$ is the wave number of the cross mode. At the leading order of secularity, the modulation amplitude ζ_1 satisfies a nonlinear Schrödinger (NLS) equation modified to include weak linear damping and weak parametric drive of frequency 2ω:[6]

$$-2i\omega(\partial\zeta_1/\partial t) + c^2(\partial^2\zeta_1/\partial x^2) + (\omega^2 - \omega_0^2 - 2i\omega\beta)\zeta_1 - 2\omega^2\eta\zeta_1^* - \Gamma\omega^2k^2|\zeta_1|^2\zeta_1 = 0\,. \tag{2}$$

The linear frequency of the cross mode is $\omega_0 = (gkT)^{1/2}$, where $T = \tanh(kh)$ and h is the depth. The damping parameter is β and the dimensionless drive amplitude is $\eta = \omega^2 a/g$, where the displacement of the drive is $a\cos(2\omega t)$ and g is the acceleration due to gravity. The nonlinear coefficient is $\Gamma = (9T^{-4} - 12T^{-2} - 3 - 2T^2)/8$, and $c^2 = (\omega_0/k)d\omega_0/dk$. The higher harmonics in the surface displacement (1), which are generated by nonlinearities, are[5]

$$\zeta_2 = k(3T^{-2} - 1)\zeta_1^2/4T\,, \qquad \zeta_2^{(0)} = k(1+T^2)|\zeta_1|^2/2T\,. \tag{3}$$

The value of the nonlinear coefficient ranges from $\Gamma = \infty$ for $kh = 0$ (shallow limit) to $\Gamma = -1$ for $kh = \infty$ (deep limit), and vanishes for $kh \simeq 1.058$. This crossover condition corresponds to a depth of 1.92 cm for our channel. When $\Gamma < 0$ the free oscillations of the cross mode *soften* (i.e., the frequency decreases as the amplitude is increased). In this case the mode is subject to the Benjamin-Feir instability,[3,7] and initial disturbances evolve into breather solitons described by hyperbolic secants. For $\Gamma > 0$ the free oscillations of the cross mode *harden* and the mode is consequently stable. However, there can exist a 180° kink in the phase of the mode. The stable kink solution to the driven damped NLS equation (2) is

$$\zeta_1 = (c\alpha/\omega k)(2/\Gamma)^{1/2}\tanh[\alpha(x - x_0)]e^{-i\delta}\,, \tag{4}$$

where $\alpha^2 = (\omega^2 - \omega_0^2 + 2\omega\mu)/2c^2$, $\tan(2\delta) = \beta/\mu$, and $\mu = (\omega^2\eta^2 - \beta^2)^{1/2}$. The location x_0 of the node of the kink is arbitrary as long as it is not near the end walls of the channel. Because of the only two possible steady-state phases consistent with a parametric drive, the driven link is topological.

The NLS equation (2) in the undriven undamped case differs formally from the standard NLS equation by the addition of the $(\omega^2 - \omega_0^2)\zeta_1$ term. This can be easily removed by transforming ζ_1 with an exponential phase factor in time. The significance of the added term is that it allows nonpropagating solutions, in which dissipation can be overcome by a global drive. In the undriven undamped case, there exists a more general single-kink solution to (2) that not only propagates at an arbitrary velocity and has a spatially varying phase, but also has an arbitrary "darkness" parameter which is simultaneously a measure of the phase difference between the two domains and the minimum amplitude of the profile.[8] As a result of this added parameter, these solitons are called dark solitons. The parameter continuously connects the kink to the (0,1) mode. Hence, unlike the damped parametrically driven kink (4), the free kink is not topological. Dark solitons have been theoretically shown to collide elastically,[9] and thus are strict solitons. Propagating kinks and dark solitons have been observed in optical fibers.[10]

The nonpropagating kink is a limiting case of a spatially periodic wave described by the elliptic function $\mathrm{sn}(p,x)$ where p is the elliptic modulus. In this solution, the tanh in (4) is replaced by sn, the amplitude is multiplied by $[2p^2/(1+p^2)]^{1/2}$, and α is multiplied by $[2/(1+p^2)]^{1/2}$. The analogous solution for the softening case involves the cn function, and the corresponding wave is referred to as a "cnoidal" wave.[6] We thus refer to the sn solution as a "snoidal" wave. We believe that our observations are the first of snoidal waves. For a wave with a single node at the center of a channel of length L, the end boundary conditions uniquely determine the value of p through the relationship

$(1+p^2)K^2(p)=L^2a/4c^2$, where $K(p)$ is the complete elliptic integral of the first kind. For low amplitudes ($p\approx 0$), the sn solution reduces to the linear (1,1) mode described by the sine function. For large amplitudes ($p\approx 1$), the sn solution reduces to the kink (4).

To compare the experimental data in Fig. 3 to the theory (1), (3), and (4), we determined the damping parameter β from the data of Fig. 4 and the parametric-drive threshold condition $\beta=\omega\eta$ at $\omega=\omega_0$. The resultant value is $\beta=0.197\ s^{-1}$ (quality factor of 42). The theoretical profile, especially for small amplitudes, is sensitive to the depth of the liquid, $h=1.00\pm 0.01$ cm. We therefore varied this value over the range of uncertainty, to achieve the best fit of the small-amplitude data in Fig. 3. The corresponding value, $h=0.996$ cm, was then used for the theoretical profile of the large-amplitude case. The small-amplitude profile has elliptic modulus $p=0.732$, and the large-amplitude profile has $p=0.998$. There is good agreement between the experiment and the above theory in the small-amplitude case, but significant deviations appear in the large-amplitude case. The solid large-amplitude curve gives the absolute maxima and minima according to the theory. The substantial asymmetry here is due to nonlinearities as manifested by the harmonic terms (3). This effect is enhanced by the shallow depth of the liquid, which causes the harmonic ζ_2 to have roughly half the amplitude of the fundamental ζ_1 in (1). Accordingly, the motion should display an "extremum doubling" in which the minima of the fundamental become relative maxima. These values are shown by the dashed curves in Fig. 3. We observe *no* such extremum doubling in the kink, although we have seen the effect in some modes of the channel.

The rich structure of the nodal region [Fig. 2(b)] is also indicative of new effects which appear beyond the NLS approximation. For example, according to (3) and (4) the minimum peak-to-peak amplitude should be zero. The structure shown in Fig. 2(b) can be qualitatively modeled by adding a term $B\,|\,\partial\zeta_1/\partial x\,|^2$ to the expression for ζ_2 in (3), where $B=-0.04/a^2A$. Terms of this form are likely to enter at higher orders of perturbation. It is doubtful, however, that a calculation of these corrections to the NLS equation will yield a satisfactory description of the large-amplitude kinks, because (a) the predicted extremum doubling is absent and (b) the amplitude of the second harmonic is comparable to that of the fundamental. Indeed, the stability of these solitary waves appears to be a more general property of nature than can be inferred from interpretations based upon the leading order, integrable (NLS), approximation to the first principles of fluid mechanics (the Euler equation or, when dissipation is included, the Navier-Stokes equation).

We are grateful to J. Ariyasu, B. Barber, A. Bishop, A. Greenfield, and G. Williams for helpful comments. This work was supported in part by DOE Grants No. FG03-87ER13686 and No. FG03-86ER45232.

[a]Current address: Department of Physics-Code PH/De, Naval Postgraduate School, Monterey, CA 93943.

[1]B. Denardo, A. Larraza, and S. Putterman, J. Acoust. Soc. Am. **84**, Suppl. 1, S34 (1988).

[2]J. Wu, R. Keolian, and I. Rudnick, Phys. Rev. Lett. **52**, 1421 (1984); J. Wu and I. Rudnick, Phys. Rev. Lett. **55**, 204 (1985).

[3]B. Denardo, Ph.D. thesis, University of California, Los Angeles, 1990 (unpublished).

[4]L. D. Landau and E. M. Lifshitz, *Mechanics* (Pergamon, New York, 1976), 3rd ed., pp. 80–83 and 90–92.

[5]A. Larraza and S. Putterman, J. Fluid Mech. **148**, 443 (1984); Phys. Lett. **103A**, 15 (1984).

[6]J. W. Miles, J. Fluid Mech. **148**, 451 (1984).

[7]R. K. Dodd, J. C. Eilbeck, J. D. Gibbon, and H. C. Morris, *Solitons and Nonlinear Wave Equations* (Academic, New York, 1982), pp. 505–506.

[8]A. Hasegawa and F. Tappert, Appl. Phys. Lett. **23**, 171 (1973).

[9]V. E. Zakharov and A. B. Shabat, Zh. Eksp. Teor. Fiz. **64**, 1627 (1973) [Sov. Phys. JETP **37**, 823 (1973)].

[10]A. M. Weiner, J. P. Heritage, R. J. Hawkins, R. N. Thurston, E. M. Kirschner, D. E. Leaird, and W. J. Tomlinson, Phys. Rev. Lett. **61**, 2445 (1988).